

## Se Isotopes as Groundwater Redox Indicators: Detecting Natural Attenuation of Se at an in Situ Recovery U Mine

Anirban Basu,<sup>\*,†,∇,^</sup> Kathrin Schilling,<sup>‡,∇</sup> Shaun T. Brown,<sup>†,§</sup> Thomas M. Johnson,<sup>||</sup> John N. Christensen,<sup>§</sup> Matt Hartmann,<sup>⊥</sup> Paul. W. Reimus,<sup>#</sup> Jeffrey M. Heikoop,<sup>#</sup> Giday Woldegabriel,<sup>#</sup> and Donald J. DePaolo<sup>†,§</sup>

<sup>†</sup>Department of Earth and Planetary Science, University of California, 307 McCone Hall, Berkeley, California 94720, United States

<sup>‡</sup>Department of Environmental Science, Policy and Management, University of California, 130 Mulford Hall, Berkeley, California 94720, United States

<sup>§</sup>Lawrence Berkeley National Laboratory, 1 Cyclotron Road, Berkeley, California 94720, United States

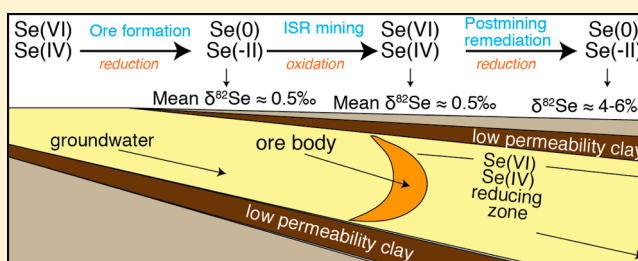
<sup>||</sup>Department of Geology, University of Illinois at Urbana–Champaign, 605 East Springfield Avenue, Champaign, Illinois 61820, United States

<sup>⊥</sup>Uranium Resources, Inc., 6950 South Potomac Street, Suite 300, Centennial, Colorado 80112, United States

<sup>#</sup>Earth and Environmental Sciences Division, Los Alamos National Laboratory, Los Alamos, New Mexico 87545, United States

### Supporting Information

**ABSTRACT:** One of the major ecological concerns associated with the in situ recovery (ISR) of uranium (U) is the environmental release of soluble, toxic selenium (Se) oxyanions generated by mining. Post-mining natural attenuation by the residual reductants in the ore body and reduced down-gradient sediments should mitigate the risk of Se contamination in groundwater. In this work, we investigate the Se concentrations and Se isotope systematics of groundwater and of U ore bearing sediments from an ISR site at Rosita, TX, USA. Our results show that selenate (Se(VI)) is the dominant Se species in Rosita groundwater, and while several up-gradient wells have elevated Se(VI), the majority of the ore zone and down-gradient wells have few or no Se oxyanions. In addition, the  $\delta^{82}\text{Se}_{\text{VI}}$  of Rosita groundwater is generally elevated relative to the U ore up to +6.14‰, with the most enriched values observed in the ore-zone wells. Increasing  $\delta^{82}\text{Se}$  with decreasing Se(VI) conforms to a Rayleigh type distillation model with an  $\epsilon$  of  $-2.25\text{‰} \pm 0.61\text{‰}$ , suggesting natural Se(VI) reduction occurring along the hydraulic gradient at the Rosita ISR site. Furthermore, our results show that Se isotopes are excellent sensors for detecting and monitoring post-mining natural attenuation of Se oxyanions at ISR sites.



### INTRODUCTION

The environmental mobility of the redox-active element Se is largely controlled by the high solubility contrast between its oxidation states. The oxidized Se species (i.e., Se(VI) and Se(IV)) are highly soluble, mobile, and toxic at elevated concentrations. Se immobilization in the environment occurs via chemical reduction to insoluble Se(0) or Se(-II). This redox-induced Se immobilization is common during the formation of roll-front uranium (U) ore deposits at redox interfaces in groundwater systems. Information about key reactions involving Se in redox-interface mineral deposits is crucial for understanding ore deposition mechanisms as well as pathways of Se cycling in aqueous environments.

Reductive immobilization of Se is an important reaction that tends to concentrate Se in roll-front type U ore deposits.<sup>1,2</sup> Commonly, ferroselite (FeSe<sub>2</sub>) and pyrite are host minerals for Se in these U ore deposits.<sup>1–4</sup> Compared to its average crustal concentration (0.05 mg/kg), high concentrations of Se ranging from 0.5–500 mg/kg are reported from the roll-front deposits in Wyoming, Montana, and Utah in the United States.<sup>5–7</sup>

These anomalously high Se concentrations have been used for U prospecting, particularly to characterize the location and shape of roll-front type deposits.<sup>8</sup> The similarity between the redox potential for reduction of Se oxyanions (Figure 1) and dissolved hexavalent uranium (U(VI))<sup>9–11</sup> leads to coprecipitation of Se minerals and U minerals.

In contrast, the oxidative dissolution of U ore enriched with Se minerals mobilizes Se and U in the environment in their toxic, oxidized forms. Se in the effluent from a traditional U mining and milling operation in northern Saskatchewan, Canada, led to the accumulation of toxic levels of Se in aquatic organisms.<sup>12,13</sup> Elevated Se concentrations in runoff or aquifers are reported from the regions of U mining and milling in the United States (e.g., Puerco River, Arizona; New Mexico; Rifle, Colorado).<sup>14,15</sup> At present, almost all recent U mining in the

Received: March 24, 2016

Revised: June 23, 2016

Accepted: August 22, 2016

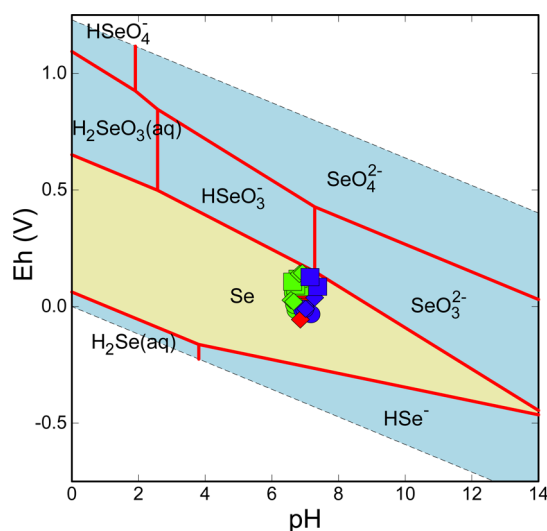


**Figure 1.** Pourbaix diagram for Se showing the thermodynamic stability of different Se species in the environment. Total Se concentration is  $10^{-6}$  M. Light blue fields represent aqueous species, and golden field represents solid Se species. Red, green, and blue symbols represent groundwater from mining units PAA 1, PAA 2, and PAA 3, respectively. Squares, circles, and diamonds represent groundwater samples from up-gradient, ore-zone, and down-gradient wells, respectively.

65 United States and  $\sim 50\%$  of global U mining employ a mining  
 66 technique known as in situ recovery (ISR) that extracts U by  
 67 oxidative dissolution of roll-front type sandstone-hosted ore  
 68 deposits.<sup>16,17</sup> Despite several advantages such as the lack of mill  
 69 tailings and radioactive dust, and its low  $\text{CO}_2$  emission  
 70 footprint, this mining method releases Se as toxic, mobile Se  
 71 oxyanions along with U(VI) directly into groundwater.<sup>18</sup>  
 72 Current strategies to mitigate Se(VI) in the groundwater after  
 73 the completion of mining include groundwater sweep and  
 74 occasionally active remediation by biostimulation or injection  
 75 of abiotic reductants.<sup>19</sup>  
 76 Understanding naturally occurring reduction of Se oxyanions  
 77 is critical for designing efficient remediation–restoration  
 78 strategies at ISR sites. Natural attenuation of U(VI) by the  
 79 existing reducing environments down-gradient of the redox  
 80 interface at roll-front deposits has been proposed as an  
 81 inexpensive but effective remediation strategy. Recent work  
 82 from our group demonstrates conditions favorable for post-  
 83 mining U(VI) reduction at ISR sites.<sup>20,21</sup> After the cessation of  
 84 mining, the residual reducing capacity of the U ore and the  
 85 prevailing reducing environments down-gradient of the ore  
 86 should reduce mine-generated elevated concentrations of toxic  
 87 Se oxyanions. At pH 7, the redox potential (Eh) required for  
 88 the reduction of Se oxyanions ( $\sim 0.4$  V for Se(VI)–Se(IV) and  
 89  $\sim 0.2$  V for Se(IV)–Se(0)) is higher than that for U(VI) ( $\sim 0.0$   
 90 V),<sup>9–11</sup> meaning that the reduction of Se(VI) and Se(IV)  
 91 should precede U(VI) reduction. The challenge is to identify  
 92 the active reduction of Se in the ore-zone or down-gradient  
 93 groundwater and distinguish reduction from other processes  
 94 that may affect aqueous Se concentration such as sorption and  
 95 dilution.

96 An effective approach to better understand important  
 97 reactions and possibly the reactions kinetics is the study of  
 98 variations in stable isotope ratios. Se reduction can be detected  
 99 by shifts in the relative abundance of its stable isotopes ( $^{82}\text{Se}$ ,  
 100  $^{80}\text{Se}$ ,  $^{78}\text{Se}$ ,  $^{77}\text{Se}$ ,  $^{76}\text{Se}$ , and  $^{74}\text{Se}$ ). The reduction of Se(VI) to

Se(0) or Se(–II) via the intermediate product Se(IV) induces a 101  
 kinetic isotopic fractionation resulting in the enrichment of 102  
 heavier isotopes (i.e.,  $^{82}\text{Se}$ ) in the remaining dissolved Se 103  
 oxyanions.<sup>11,22–24</sup> This enrichment is described in terms of an 104  
 isotopic enrichment factor  $\epsilon$ , a per mil quantity, expressed as 105

$$\epsilon = 1000\text{‰} \times (\alpha - 1) \quad (1) \quad 106$$

where  $\alpha$  is the isotopic fractionation factor, defined as 107  
 $\alpha = \frac{R_{\text{product}}}{R_{\text{reactant}}}$ , and  $R_{\text{product}}$  and  $R_{\text{reactant}}$  are the  $^{82}\text{Se}/^{76}\text{Se}$  in the 108  
 reduction product and remaining Se oxyanions, respectively. 109  
 Relatively large isotopic fractionation factors are observed 110  
 during microbial reduction of Se(VI) to Se(IV) ( $\epsilon \sim -8\text{‰}$ ) 111  
 and of Se(IV) to elemental Se ( $\epsilon \sim -14\text{‰}$ ).<sup>25</sup> Abiotic 112  
 reduction of Se(VI) by green rust or of Se(IV) by FeS also 113  
 induces large fractionations (up to  $-11\text{‰}$ ).<sup>22,23,26</sup> In contrast, 114  
 adsorption of Se(IV) to mineral surfaces results in a smaller 115  
 fractionation ( $\sim -1\text{‰}$ ).<sup>26,27</sup> Thus, Se stable isotope ratios in 116  
 groundwater are a more reliable indicator of reduction of Se 117  
 oxyanions than aqueous concentrations of the Se species, which 118  
 are less easy to interpret because of the effects of dilution, 119  
 removal by adsorption, or advection of heterogeneous plumes 120  
 past sampling points.

Although the release of potentially toxic Se oxyanions by ISR 121  
 activity is a widespread environmental risk, the fate of mobilized 122  
 Se at post-mining ISR sites is not yet well-understood. In this 123  
 article, we present species-specific Se concentrations and 124  
 isotopic measurement data for U ore and 33 groundwater 125  
 samples collected from wells located up-gradient, within, and 126  
 down-gradient of a roll-front deposit located at an ISR site at 127  
 Rosita, TX, USA. Sample locations include both previously 128  
 mined and unmined parts of the site. The objective of our study 129  
 is to demonstrate naturally occurring Se oxyanion reduction at 130  
 the site using Se isotope ratios of groundwater samples 131  
 collected across a groundwater redox interface. In addition, we 132  
 discuss how the Se isotope data may provide additional 133  
 information about the redox condition in the aquifer, 134  
 particularly in the unmined part of the site, in relation to 135  
 other geochemical indicators (i.e., Se concentrations, U 136  
 concentrations, and U isotope data). 137

## 138 ■ MATERIALS AND METHODS

**Site Description and Groundwater Sampling.** The 139  
 study site is located at Rosita, TX, USA (Figure 2). A detailed 140  
 description of the site can be found in Basu et al., 2015.<sup>20</sup> 141  
 Briefly, the U roll-front deposit at this ISR site is defined by a 142  
 poorly consolidated, mineralized sand unit bounded above and 143  
 below by low-permeability clay units. For ISR mining, site 144  
 groundwater fortified with  $\text{O}_2$  and  $\text{H}_2\text{O}_2$  was injected into the 145  
 ore zone in three mining units or production area author- 146  
 izations (PAA) to oxidize and dissolve the U ore utilizing the 147  
 high natural bicarbonate concentrations to stabilize U– $\text{CO}_3$  148  
 complexes. The mining unit PAA 4 has a complete set of 149  
 monitoring wells, but no mining has occurred to date. The 150  
 mining was followed by a restoration process except in the 151  
 most recently mined PAA 3, where the site groundwater treated 152  
 by reverse osmosis was injected back into the aquifer. A 153  
 network of existing wells, drilled within and up-gradient and 154  
 down-gradient of the ore body, was used for post-mining 155  
 monitoring of the site. The baseline (BL) wells located within 156  
 the production zone was used for monitoring the water quality 157  
 in the ore zone, while the up-gradient and down-gradient 158  
 monitoring wells (MW) were used to ensure that there was no 159

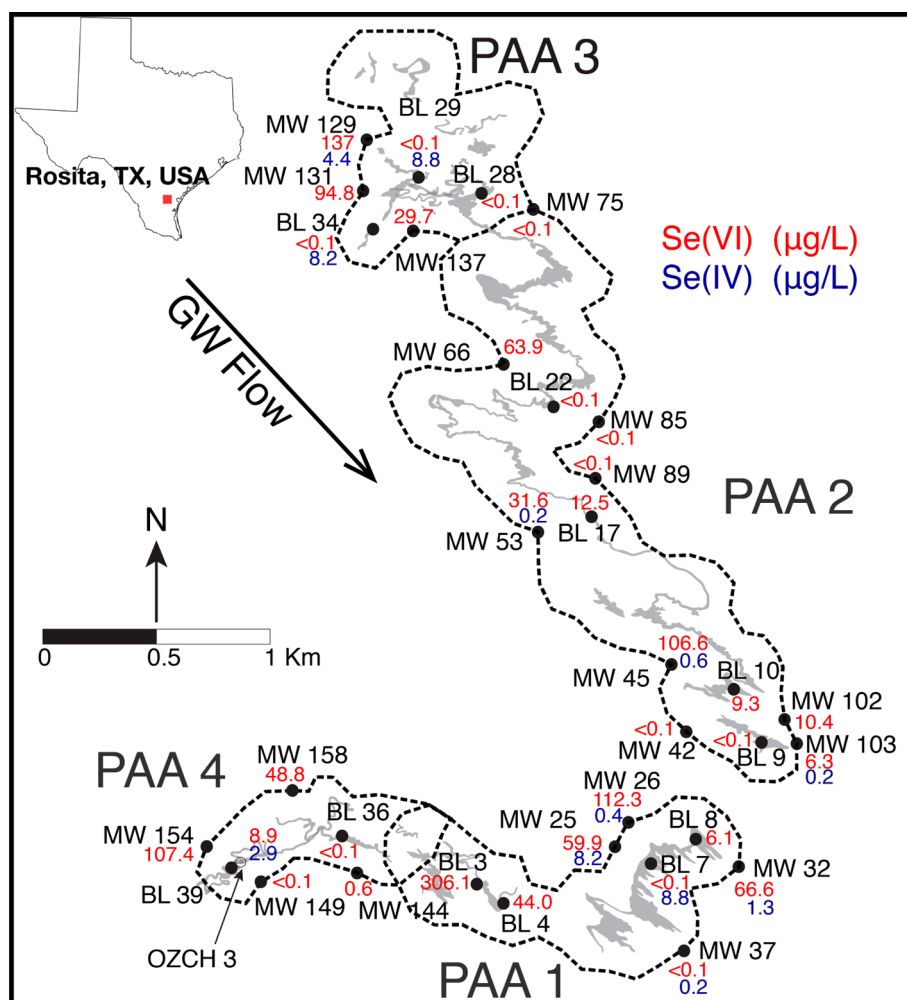


**Figure 2.** Map of the Rosita ISR site showing the mining units (PAA) and the distribution of Se(VI). Light gray areas define the roll-front U deposit. Black dots represent locations of wells sampled for Se oxyanion and Se isotope measurements, and the open circle shows the location of the borehole for the U ore sample. The dotted lines represent the perimeter ring of the monitoring wells. Numbers represent Se oxyanion concentrations, Se(VI) (red) and Se(IV) (blue) in  $\mu\text{g/L}$ .

160 excursion of the mining or restoration fluid leaving the ore  
161 zone.

162 Groundwater samples were collected from 33 wells along  
163 transects roughly parallel to the current groundwater flow  
164 direction. The wells were purged prior to sampling, and  
165 samples for Se oxyanion concentrations and Se isotopes were  
166 filtered using  $0.45\ \mu\text{m}$  in-line filters and collected in precleaned  
167 HDPE bottles with no headspace and no preservatives. The  
168 samples were stored at  $4\ ^\circ\text{C}$  prior to analysis.

169 **Sediment Digestion.** U ore samples were obtained from a  
170 borehole (OZCH 3) adjacent to BL 39 in PAA 4 (Figure 2).  
171 For Se concentration and isotopic analysis, 1.0 g aliquots of  
172 sediment samples from seven discrete depths were digested in  
173 an acid mixture (concentrated HCl + concentrated  $\text{HNO}_3$ , 3:1  
174 v/v). First, each 1.0 g aliquot was treated with 4 mL of  $\sim 7\ \text{M}$   
175  $\text{HNO}_3$  in Teflon beakers at  $80\ ^\circ\text{C}$  for about 12 h to remove any  
176 carbonate from the sediments. The remaining  $\text{HNO}_3$  was then  
177 evaporated to near-dryness at  $60\ ^\circ\text{C}$  prior to addition of a  
178 freshly prepared acid mixture of HCl and  $\text{HNO}_3$ . The samples  
179 were digested at  $80\ ^\circ\text{C}$  for 24 h. After digestion, the acid  
180 mixture was removed by evaporating to near-dryness at  $70\ ^\circ\text{C}$ ,  
181 and 5 mL of 0.1 N HCl was added. This solution was filtered  
182 using  $0.45\ \mu\text{m}$  PTFE filters to remove undigested particles.

**Sample Purification and Mass Spectrometry.** Se isotope ratios were measured using multicollector inductively coupled plasma mass spectrometry (MC-ICP-MS) at the Department of Geology, University of Illinois, Urbana-Champaign following the methods described in Schilling et al., 2014 and 2015.<sup>28,29</sup> For isotopic measurements, we used a double spike technique ( $^{74}\text{Se} + ^{77}\text{Se}$ ) to correct for the isotopic fractionation during mass spectrometry and any that might occur during sample purification by ion exchange chromatography.<sup>28,29</sup> An aliquot of the double-spike solution of appropriate species (either Se(IV) or Se(VI)) was added to a carefully weighed aliquot of the sample (groundwater or digested U ore) containing approximately 100 ng of Se.

The Se oxyanion species was purified from other Se species and matrix elements by ion exchange chromatography.<sup>29</sup> For the separation of Se(VI), the samples were first acidified with HCl to a final strength not exceeding 0.1 M HCl. The acidified samples were passed through the anion exchange resin (Eichrom Technologies LLC, Lisle, IL), where Se(VI) was adsorbed onto the resin, while Se(IV) and other matrix elements (e.g., As and Ge) were rinsed out with 0.1 M HCl. Se(VI) was eluted from the resin by 6 M HCl and heated to  $105\ ^\circ\text{C}$  for 1 h. Finally, the samples were diluted to 2 M HCl, 205

Table 1. Se Concentrations and Isotope Ratios in Rosita Groundwater and U Ore<sup>a</sup>

Rosita groundwater							
well	location	PAA	Se(VI) $\mu\text{g/L}$	$\delta^{82}\text{Se}_{\text{VI}}$	Se(IV) $\mu\text{g/L}$	$\delta^{82}\text{Se}_{\text{IV}}$	Eh (mV)
BL 3	ore zone	1	306.06	-1.46‰	<0.1		
BL 4	ore zone	1	44.02	0.97‰	<0.1		-6.0
BL 7	ore zone	1	<0.1		8.61	-1.36‰	-37.5
BL 8	ore zone	1	6.08	0.82‰	<0.1		46.4
BL 9	ore zone	2	<0.1		<0.1		9.2
BL 10	ore zone	2	9.32	0.97‰	<0.1		81.2
BL 17	ore zone	2	12.51	5.19‰	<0.1		-64.5
BL 22	ore zone	2	<0.1		<0.1		-42.6
BL 28	ore zone	3	<0.1		<0.1		-62.7
BL 29	ore zone	3	<0.1		3.18	0.51‰	-82.5
BL 34	ore zone	3	<0.1		8.22	0.73‰	-59.4
MW 25	up-gradient	1	59.87	0.58‰	8.17	-2.92‰	23.3
MW 26	up-gradient	1	112.27	0.9‰	0.4	ND	56.5
MW 32	down-gradient	1	66.56	0.45‰	1.29	-6.45‰	56.1
MW 37	down-gradient	1	<0.1		0.15	-2.63‰	-105.5
MW 42	up-gradient	2	<0.1		<0.1		34.0
MW 45	up-gradient	2	106.62	-0.47‰	0.61	ND	69.5
MW 53	up-gradient	2	31.59	0.83‰	0.24	ND	40.5
MW 66	up-gradient	2	63.87	0.7‰	<0.1		56.5
MW 75	down-gradient	3	<0.1		<0.1		-11.7
MW 85	down-gradient	2	<0.1		<0.1		-22.3
MW 89	down-gradient	2	<0.1		<0.1		-29.0
MW 102	down-gradient	2	10.38	1.12‰	<0.1		90.2
MW 103	down-gradient	2	6.26	0.59‰	0.2	-4.66‰	94.2
MW 129	up-gradient	3	137.01	0.43‰	4.35	-3.69‰	35.4
MW 131	up-gradient	3	94.84	0.54‰	<0.1		76.5
MW 137	down-gradient	3	29.72	0.51‰	<0.1		-59.5
BL 36	ore zone	4	<0.1		<0.1		
BL 39	ore zone	4	8.97	6.14‰	2.87	-0.61‰	
MW 144	down-gradient	4	0.6	ND	<0.1		
MW 149	down-gradient	4	<0.1		<0.1		
MW 154	up-gradient	4	107.44	2.22‰	<0.1		
MW 158	up-gradient	4	48.83	-1.12‰	<0.1		
Rosita U ore							
depth below ground surface (m)			Se ( $\mu\text{g/kg}$ )	$\delta^{82}\text{Se}$			
60.66–60.96 (background)			24.3	-1.54‰			
66.14–66.45			36.8	-1.28‰			
66.45–66.75			33.8	-0.85‰			
66.75–67.06			30.8	-0.62‰			
67.06–67.21			31.7	-0.79‰			
70.71–71.02			47.6	-0.64‰			
71.02–71.32			39.0	-0.40‰			

<sup>a</sup>ND: not determined. Eh measurements are from Basu et al., 2015.

206 sparged with  $\text{N}_2$  to remove a volatile Br species, and  
207 equilibrated with Kr in the air for 12 h prior to isotopic analysis.

208 For Se(IV) extraction, the samples were not acidified before  
209 loading on the anion exchange resin. The Se(VI) was adsorbed  
210 onto the resin, and the effluent containing Se(IV) was collected  
211 by rinsing with 0.1 M HCl and then oxidized to Se(VI) by  
212 treatment with  $\text{K}_2\text{S}_2\text{O}_8$  at 100 °C for 1 h. After oxidation, all  
213 samples were purified using the above procedure for Se(VI)  
214 purification.

215 For purification of Se from the digested U ore (as Se(IV)),  
216 we first evaporated the samples to near-dryness and then  
217 redissolved them in 5 mL of 0.1 M HCl. An aliquot of this  
218 solution containing ~100 ng of Se was brought to a strength of  
219 4–6 M HCl prior to purification by hydride generation

described in ref 30. The  $\text{H}_2\text{Se}$  was trapped in a mixture of 220  
NaOH and  $\text{H}_2\text{O}_2$  and converted to Se(VI). The excess  $\text{H}_2\text{O}_2$  221  
was removed from the samples by heating (~100 °C) prior to 222  
purification using the procedure for Se(VI) described above. 223

Se isotope ratios are reported as  $\delta^{82}\text{Se}$  relative to the isotopic 224  
standard reference material NIST SRM 3149,<sup>31</sup> defined as 225

$$\delta^{82}\text{Se} = \left[ \frac{(^{82}\text{Se}/^{76}\text{Se})_{\text{sample}}}{(^{82}\text{Se}/^{76}\text{Se})_{\text{SRM3149}}} - 1 \right] \times 1000\text{‰} \quad (2)$$

The uncertainty ( $2\sigma$ ) of  $\delta^{82}\text{Se}$  measurements, calculated from 227  
the twice the root mean square (RMS, 95% confidence level)<sup>32</sup> 228  
of 24 duplicate sample preparations and analysis, was 0.17‰. 229  
The value of the isotopic fractionation factor ( $\alpha$ ) was 230



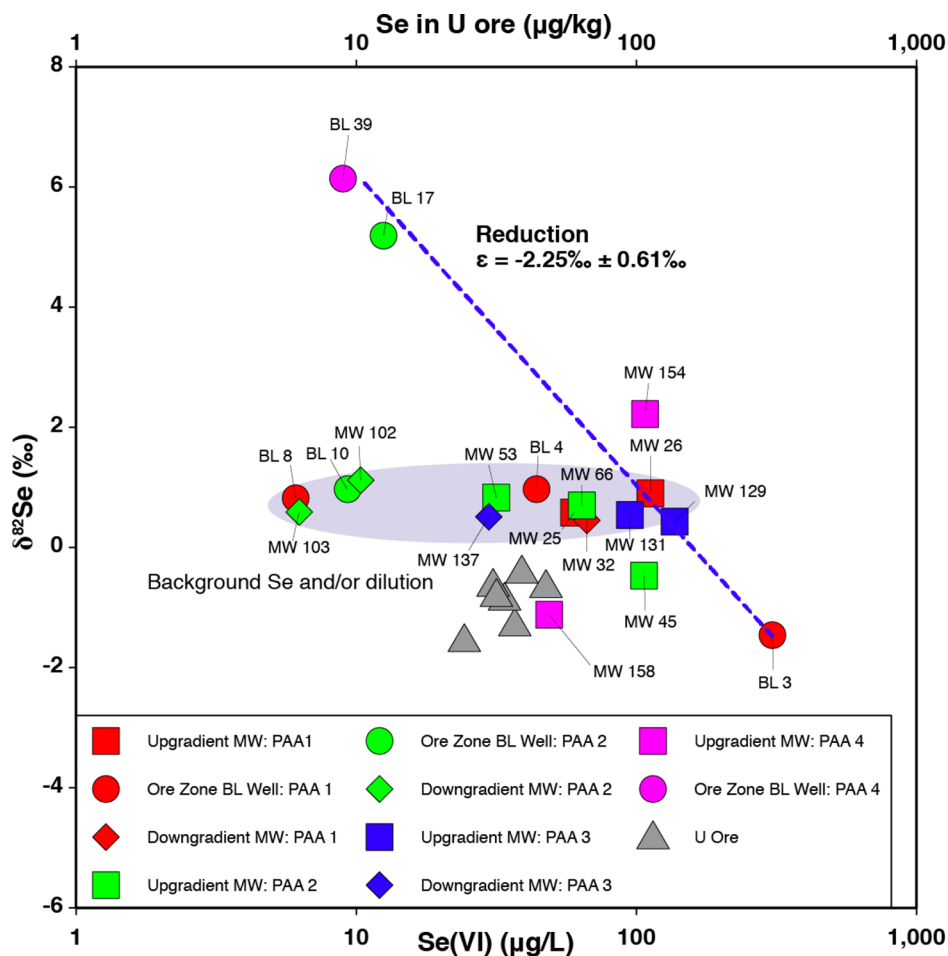


**Figure 3.**  $\delta^{82}\text{Se}$  of aqueous Se(VI) in Rosita groundwater and Se minerals in the U ore vs Se concentration. Gray triangles represent the U ore, and red, green, blue, and pink symbols represent groundwater from mining units PAA 1, PAA 2, PAA 3, and PAA 4, respectively. The error bars ( $2 \times \text{SE}$ ) are smaller than the size of the symbols. The blue dotted line represents the modeled  $\delta^{82}\text{Se}$  using a Rayleigh distillation model with  $\epsilon = -2.25\text{‰} \pm 0.61\text{‰}$ , excluding the samples with  $\text{NO}_3^-$ .

231 determined from the slope of the best-fit line from the  
 232 linearized plot of  $\ln(\delta^{82}\text{Se} + 1000\text{‰})$  versus  $\ln(\text{Se(VI)})$ .<sup>33</sup> The  
 233 uncertainties ( $2\sigma$ ) of  $\epsilon$  were  $\pm 0.6\text{‰}$ , calculated from the scatter  
 234 of the data points around the best-fit line using standard linear  
 235 estimation methods.

## 236 ■ RESULTS AND DISCUSSION

### 237 Se Concentrations in Rosita Groundwater and U Ore.

238 We have quantified Se(VI) and Se(IV) concentrations in the  
 239 Rosita groundwater (Table 1) to understand the distribution  
 240 pattern of the aqueous Se species at the study site. Se(VI) is the  
 241 dominant species with concentrations up to  $306 \mu\text{g/L}$  in the  
 242 groundwater samples, while Se(IV) is found in fewer samples  
 243 and only at concentrations below  $9 \mu\text{g/L}$ . Generally, except for  
 244 ore-zone wells BL 3 and BL 4, groundwater from the up-  
 245 gradient monitoring wells has higher Se(VI) compared to that  
 246 in the ore-zone or down-gradient monitoring wells. We did not  
 247 observe any systematic pattern in the distribution of Se(IV) at  
 248 the site. Out of 12 samples with measurable Se(IV), three ore-  
 249 zone wells (BL 7, BL 29, and BL 34) and one down-gradient  
 250 well, MW 37, contain only Se(IV), while the rest contain both  
 251 Se(VI) and Se(IV). In the previously mined parts of the site,  
 252 the down-gradient monitoring wells MW 37, MW 75, MW 85,  
 253 and MW 89, contain little ( $<1 \mu\text{g/L}$ ) or no Se oxyanions, either  
 254 as Se(VI) or Se(IV). The wells MW 32, MW 102, MW 103,

and MW 137, located directly down-gradient of the mapped  
 255 discontinuities of the ore body (Figure 2), contain substantial  
 256 amount of Se(VI) and, in some cases, Se(IV). In the unmined  
 257 PAA 4, the down-gradient wells show little dissolved Se: MW  
 258 149 has no Se oxyanions, whereas MW 144 contains  $0.6 \mu\text{g/L}$   
 259 Se(VI) and Se(IV) below detection level ( $<0.1 \mu\text{g/L}$ ).  
 260

The Se concentrations in the U ore collected at seven  
 261 discrete depths from borehole OZCH 3 adjacent to the ore-  
 262 zone well BL 39 in the unmined PAA 4 area are low and vary  
 263 from 24 to  $48 \mu\text{g/kg}$  (Table 1). There is no apparent trend in  
 264 the Se concentrations with depth. However, the samples with  
 265 the highest U concentrations collected from 70.71–71.32 m  
 266 below the ground surface also contain the highest amount of  
 267 Se. The U ore was not characterized for the identity of Se  
 268 bearing minerals, but previous work identified ferroselite and  
 269 elemental Se as the dominant Se-bearing species in South Texas  
 270 and other roll-front type U deposits.<sup>1,2,34–37</sup>  
 271

### 272 Se Isotope Ratios in Rosita Groundwater and U Ore.

The  $\delta^{82}\text{Se}$  in groundwater samples from all PAAs and in the U  
 273 ore are provided in Table 1. The  $\delta^{82}\text{Se}$  of aqueous Se(VI) varies  
 274 from  $-1.46\text{‰}$  to  $+6.14\text{‰}$ , with most of the samples showing  
 275 elevated  $\delta^{82}\text{Se}$  relative to the Se isotope standard SRM 3149  
 276 (i.e.,  $\delta^{82}\text{Se} > 0.0\text{‰}$ ) (Figure 3). The highest  $\delta^{82}\text{Se}$  of Se(VI)  
 277 is observed in groundwater from the ore-zone well BL 39 from  
 278 the unmined PAA 4 area, while BL 3 from the already-mined  
 279

280 PAA 1 exhibits the most-depleted  $\delta^{82}\text{Se}$  value ( $-1.46\%$ ). In a  
281 subset of samples, there is an apparent trend of increasing  
282  $\delta^{82}\text{Se}_{\text{VI}}$  with decreasing Se(VI) (Figure 3). Contrary to the  
283  $\delta^{82}\text{Se}$  values of Se(VI),  $\delta^{82}\text{Se}$  of Se(IV) is substantially depleted  
284 by up to  $-6.45\%$  except in samples from BL 29 ( $\delta^{82}\text{Se}_{\text{IV}} =$   
285  $0.51\%$ ) and BL 34 ( $\delta^{82}\text{Se}_{\text{IV}} = 0.73\%$ ). Notably, these wells  
286 had no measurable Se(VI). In the samples containing both Se  
287 oxyanion species, Se(IV) is isotopically lighter than Se(VI) with  
288  $\Delta^{82}\text{Se}$  ( $\approx \delta^{82}\text{Se}_{\text{VI}} - \delta^{82}\text{Se}_{\text{IV}}$ ) ranging from  $3.5\%$  to  $6.9\%$ . We  
289 observe a weak correlation between Se(IV) concentration and  
290  $\delta^{82}\text{Se}_{\text{IV}}$  of the groundwater samples; the  $\delta^{82}\text{Se}_{\text{IV}}$  decreases with  
291 decreasing Se(IV) (Figure S1).

292 The Se isotope compositions of the Se minerals in the U ore  
293 from seven discrete depths are provided in Table 1. The  $\delta^{82}\text{Se}$   
294 of the U ore ranges from  $-1.28\%$  to  $-0.40\%$ . The median  
295 value of  $-0.72\%$  is low relative to those of the majority of the  
296 groundwater Se(VI) samples (Figure 3). There is also an  
297 enrichment in  $\delta^{82}\text{Se}$  in the ore with increasing depth.

### 298 Implication of Se Isotopic Signature of Rosita U Ore.

299 Our observations of  $^{82}\text{Se}$  depletion of the ore are limited to a  
300 single borehole (OZCH 3) in PAA 4, which does not provide  
301 the full extent of the spatial variability in  $\delta^{82}\text{Se}$  of the ore body.  
302 Furthermore, the U ore samples from the borehole OZCH 3  
303 are not representative of the Se-enriched portion of the roll-  
304 front system generated by reductive precipitation of Se. Lower  
305 Se concentrations of the U ore compared to that of up-gradient  
306 groundwater suggest a Se-rich sediment up-gradient of the  
307 borehole OZCH 3 (Table 1 and Figure 3). This is further  
308 supported by our observation of  $^{82}\text{Se}$  depletion in the U ore.  
309 Ideally, reductive precipitation of Se oxyanions at the redox  
310 interface should produce  $^{82}\text{Se}$ -depleted Se minerals at the up-  
311 gradient fringe of the roll-front deposit. With increasing  
312 distance along the hydraulic gradient, the Se minerals should  
313 become isotopically heavier. However, after complete removal  
314 of Se oxyanions from the groundwater, the Se concentrations  
315 and isotopic composition of the sediments should return to  
316 background values. The sediments collected 6 m above the ore-  
317 bearing zone contain  $24.3 \mu\text{g}/\text{kg}$  of Se with a  $\delta^{82}\text{Se}$  of  $-1.54\%$ ,  
318 resembling the ore-zone sediments both in terms of Se  
319 concentrations and isotopic composition (Table 1). Therefore,  
320 we surmise that Se concentrations and isotopic compositions of  
321 our U ore samples reflect the primary Se content of the aquifer  
322 sediments.

323 **Se Reduction in Groundwater: Se Concentration**  
324 **Distribution and Geochemical Conditions.** The distribu-  
325 tion of dissolved Se in Rosita groundwater is consistent with  
326 reduction of Se oxyanions, particularly Se(VI) reduction, by  
327 naturally occurring reducing environments within and down-  
328 gradient of the ore zone. The Se(VI) hotspots at the up-  
329 gradient wells or ore-zone wells in the mined part of the site  
330 resulted from the oxidation of Se minerals, either during mining  
331 or by interaction with the oxygenated recharge water. For  
332 example, high Se(VI) up to  $107 \mu\text{g}/\text{L}$  in the up-gradient wells  
333 MW 158 and MW 154 in the unmined PAA 4 is likely to reflect  
334 natural dissolution of Se minerals in the aquifer. In the absence  
335 of any Se removal within or down-gradient of the ore zone, the  
336 down-gradient wells should show Se(VI) concentrations similar  
337 to that of the up-gradient wells. Few or no Se oxyanions in the  
338 down-gradient wells, particularly in MW 37, MW 75, MW 85,  
339 and MW 89, suggests Se removal before groundwater arrives at  
340 these wells.

341 The observed removal of Se along the hydraulic gradient  
342 suggests the geochemical conditions conducive to reduction of

Se oxyanions within and down-gradient of the ore zone. At the  
343 study site, a progression from nitrate-reducing to Fe(III)-  
344 reducing and then to U(VI)-reducing conditions along the  
345 hydraulic gradient is inferred from concentrations of the redox  
346 species (e.g.,  $\text{NO}_3^-$ , Fe(II), and U(VI)), Eh values, and isotopic  
347 measurements (e.g.,  $\delta^{15}\text{N}$ , and  $\delta^{238}\text{U}$ ) of groundwater  
348 samples.<sup>20</sup> Briefly, a general decrease in  $\text{NO}_3^-$  concentrations  
349 along the hydraulic gradient and a linear relation between the  
350  $\delta^{18}\text{O}$ -nitrate and  $\delta^{15}\text{N}$ -nitrate ( $r^2 = 0.77$ ,  $n = 11$ ) with a slope  
351 ( $\Delta\delta^{18}\text{O}/\Delta\delta^{15}\text{N}$ ) of  $0.73 \pm 0.13$  is indicative of microbial  
352 denitrification. In addition, localized zones of Fe(III) and  
353 Mn(IV) reduction is suggested by elevated dissolved Mn  
354 ( $>0.05 \text{ mg}/\text{L}$ ) and Fe ( $>0.1 \text{ mg}/\text{L}$ ) concentrations in  
355 groundwater samples from PAA 1, PAA 2, and PAA 3.  
356 Furthermore, decreasing Eh of samples down-gradient of the  
357 ore zone (except MW 32, MW 102, MW 103, and MW 137) in  
358 all previously mined PAAs, also consistent with the pattern  
359 observed for redox-sensitive aqueous species. Among the down-  
360 gradient wells investigated by Basu et al. (2015), the samples  
361 from MW 37, MW 75, MW 85, and MW 89 exhibited low Eh  
362 ( $-11.7$  to  $-105.5 \text{ mV}$ ), low U(VI) concentrations ( $<20 \mu\text{g}/\text{L}$ )  
363 and highly depleted  $\delta^{238}\text{U}$  ( $-1.41\%$  to  $-2.49\%$ ) suggesting  
364 naturally occurring reducing environments capable of U(VI)  
365 and thus, Se(VI) reduction. 366

The overall range of Eh and pH suggests thermodynamic  
367 favorability of Se oxyanions reduction in Rosita groundwater  
368 (Figure 1). The decrease in Se(VI) along the hydraulic gradient  
369 is therefore consistent with the Se(VI) and perhaps Se(IV)  
370 reduction down-gradient of the ore zone suggested by Basu et  
371 al. 2015 on the basis of U isotopes and other evidence. 372  
Alternatively, Se(IV) could be strongly adsorbing and removed  
373 via sorption onto minerals. 374

Several down-gradient wells, however, do not follow the  
375 general trend of aqueous Se(VI) removal along the hydraulic  
376 gradient. These wells, MW 32, MW 102, MW 103, and MW  
377 137, are located directly down-gradient of the mapped gaps in  
378 the ore body (Figure 2). These gaps may mark regions that  
379 lacked the reducing materials that were responsible for the  
380 formation of the ore body in the adjacent areas. This difference  
381 implies an unrestricted flow of the up-gradient water rich in  
382 Se(VI) and other oxidants (e.g.,  $\text{NO}_3^-$ ) (Figure S2) and with a  
383 high Eh to the down-gradient wells MW 32, MW 102, MW  
384 103, and MW 137 through these gaps, which conforms to the  
385 observations reported in ref 20. The post-mining restoration  
386 fluid with high residual Se(VI) is unlikely to arrive at the down-  
387 gradient wells due to low groundwater velocity ( $3\text{--}6 \text{ m}/\text{year}$ )  
388 and restriction of flow by net withdrawal of groundwater during  
389 restoration. However, the presence of the reduction product  
390 Se(IV) in MW 32 and MW 103 suggest existing Se(VI)-  
391 reducing conditions in these wells, which is also supported by  
392 our Se isotope data (see below). 393

**Se Reduction in Groundwater: Se Isotope Ratios.** If all  
394 of the variation of  $\delta^{82}\text{Se}$  were due to reduction of Se from a  
395 single Se source by a single mechanism, a strong correlation  
396 between  $\delta^{82}\text{Se}$  and concentrations of Se oxyanions would be  
397 expected. We did not observe a strong correlation between  
398  $\delta^{82}\text{Se}$  and Se(VI) concentrations, which suggests heterogeneous  
399 Se sources and complex Se cycling mechanisms. However, the  
400 samples that exhibit highly enriched  $\delta^{82}\text{Se}$  (e.g.,  $\delta^{82}\text{Se} > 4\%$ )  
401 can only be generated by reduction of Se(VI). In the following  
402 paragraphs, we discuss the evidence of Se(VI) reduction from  
403 the  $\delta^{82}\text{Se}$  data from Rosita groundwater along with potential  
404 alternative mechanisms with their limitations. 405

406 In addition to the distribution of Se oxyanion concentrations,  
407 Se isotope data from Rosita U ore and groundwater samples  
408 help identify pathways of Se cycling and delineate Se(VI)-  
409 reducing zones at the study site. The up-gradient groundwater  
410 currently entering the roll-front system is Se(VI)-rich, with  
411 concentrations ranging from 32 to 137  $\mu\text{g/L}$  (median Se(VI) =  
412 94.84  $\mu\text{g/L}$ ). The  $\delta^{82}\text{Se}$  of the up-gradient groundwater also  
413 varies from  $-1.12\text{‰}$  to  $+2.22\text{‰}$ , with an average  $\delta^{82}\text{Se}$  of  
414  $0.51\text{‰}$ . Because the roll-front system reduces and captures all  
415 incoming Se(VI), we hypothesize that the average  $\delta^{82}\text{Se}$  of the  
416 U ore should be identical to the average  $\delta^{82}\text{Se}$  of incoming  
417 groundwater, assuming that the Se inputs for the U ore were  
418 similar to that observed in the present system.

419 If dissolution of Se minerals were the only mechanism  
420 responsible for the observed distribution of Se(VI) in Rosita  
421 groundwater, we would expect the groundwater samples to be  
422 similar to the inferred average  $\delta^{82}\text{Se}$  of the U ore ( $\sim 0.5\text{‰}$ ).  
423 The oxidative dissolution of U ore should yield aqueous Se(VI)  
424 with similar isotopic composition, as quantitative layer-by-layer  
425 dissolution of Se mineral grains results in negligible isotopic  
426 fractionation. However, it is possible for the post-mining  
427 groundwater to acquire Se with a range of  $\delta^{82}\text{Se}$  values (e.g.,  $-$   
428  $1.5\text{‰}$  to  $\sim 2\text{‰}$ ) because we expect the isotopic composition of  
429 Se minerals to exhibit spatial variability in the ore zone.  
430 Aqueous Se isotope compositions outside the  $-1.5\text{‰}$  to  
431  $+2.0\text{‰}$  range suggest an alternate or additional process  
432 affecting the Se isotope composition of the groundwater.

433 The enrichments in  $\delta^{82}\text{Se}$  of Rosita groundwater relative to  
434 the inferred average  $\delta^{82}\text{Se}$  of the U ore are likely caused by  
435 Se(VI) reduction in Rosita groundwater. With ongoing  
436 reduction of Se(VI), the unreacted remaining Se(VI) exhibits  
437  $^{82}\text{Se}$  enrichment,<sup>11,22–27,30</sup> while the intermediate product  
438 Se(IV) is first enriched in the lighter isotopes (i.e.,  $^{76}\text{Se}$ ) and  
439 later, upon further reduction to Se(0) and possibly complete  
440 removal of Se(VI), is enriched in  $^{82}\text{Se}$ . The largest  $^{82}\text{Se}_{\text{VI}}$   
441 enrichments observed in the ore-zone wells BL 17 and BL 39  
442 are  $5.19\text{‰}$  and  $6.14\text{‰}$ , respectively, suggesting a maximum  
443 offset of  $\sim 6\text{‰}$  from that of the inferred  $\delta^{82}\text{Se}$  of the U ore. In  
444 all samples containing both Se(VI) and Se(IV), Se(IV) is  
445 isotopically lighter (i.e., enriched in  $^{76}\text{Se}$ ,  $-6.38\text{‰} < \delta^{82}\text{Se} <$   
446  $0\text{‰}$ ). This suggests that Se(IV) is a product of Se(VI)  
447 reduction rather than arising from the oxidation of the U ore. In  
448 addition, the two groundwater samples with  $^{82}\text{Se}_{\text{IV}}$  enrichment  
449 (i.e.,  $\delta^{82}\text{Se}_{\text{IV}} > 0\text{‰}$ ) have low Eh values ( $\text{Eh}_{\text{BL } 29} = -82.5 \text{ mV}$   
450 and  $\text{Eh}_{\text{BL } 34} = -59.4 \text{ mV}$ ) and no detectable Se(VI). This  $^{82}\text{Se}$   
451 enrichment in Se(IV) and a lack of Se(VI) suggests that  
452 extensive reduction of Se(IV) has occurred in the absence of  
453 production of Se(IV) via Se(VI) reduction.

454 The correlation between Se isotopic shifts and changes in Se  
455 oxyanion concentrations also suggests aqueous Se(VI)  
456 reduction. When Se(VI) data from all wells are pooled  
457 together, we observe two distinct trends in the relationship  
458 between  $\delta^{82}\text{Se}$  values and Se(VI) concentrations (Figure 2).  
459 First, there is an increasing trend in  $\delta^{82}\text{Se}$  with decreasing  
460 Se(VI). Second, for several wells such as BL 8, BL 10, MW 102,  
461 MW 103, MW 53, and MW 137, Se(VI) concentrations  
462 decrease with no major shift in the  $\delta^{82}\text{Se}$ . In samples showing  
463 no major change in  $\delta^{82}\text{Se}$ , particularly in BL 8, BL 10, MW 102,  
464 and MW 103, the decrease in Se(VI) may be attributed to a  
465 localized mixing with groundwater with relatively low Se,  
466 similar to that of MW 42, which is also consistent with  
467 relatively high Eh values and  $\text{NO}_3^-$  concentrations (Figure S2)  
468 in these wells.<sup>20</sup> Alternatively, a more likely scenario is that

these samples may have acquired variable amounts of Se from 469  
the Se-rich zone in the roll-front, with a  $\delta^{82}\text{Se}$  similar to the 470  
inferred average  $\delta^{82}\text{Se}$  of the roll-front. The first trend in which 471  
 $\delta^{82}\text{Se}$  in a subset of samples increased with decreasing Se(VI) 472  
conforms to a Rayleigh-type fractionation model with  $\epsilon =$  473  
 $-2.25\text{‰} \pm 0.61\text{‰}$  calculated excluding Se data from the wells 474  
containing measurable  $\text{NO}_3^-$ . This strongly suggests Se(VI) 475  
reduction as the primary mechanism of Se(VI) concentration 476  
decrease in these samples. 477

A pair of alternative mechanisms, mixing and equilibrium 478  
isotopic exchange, with the potential to influence the Se 479  
isotopic signature of Rosita groundwater are unlikely to play 480  
any major role at the study site. The elevation in  $\delta^{82}\text{Se}$  of 481  
Se(VI) in BL 39 and BL 17 above  $\sim 2\text{‰}$  cannot be generated 482  
by mixing ore-zone groundwater with an average  $\delta^{82}\text{Se}$  of 483  
 $0.5\text{‰}$ , with the up-gradient water entering the system with a 484  
maximum  $\delta^{82}\text{Se}$  of  $\sim 2\text{‰}$ . Therefore, mixing cannot account for 485  
the observed elevated  $\delta^{82}\text{Se}$  values of Se(VI) in BL 39 and BL 486  
17. Also, an equilibrium isotopic exchange between coexisting 487  
dissolved species Se(VI) and Se(IV) or more reduced Se 488  
species would lead to  $^{82}\text{Se}$  enrichment in Se(VI). This seems 489  
highly unlikely under the prevalent geochemical conditions that 490  
are far from chemical equilibrium. The rates of exchange 491  
between Se(VI) and Se(IV), which requires the transfer of two 492  
electrons, have yet to be determined. However, on the basis of 493  
recent reports on U(VI)–U(IV) exchange also requiring two 494  
electrons transferred,<sup>38</sup> very slow exchange (100 to 1000 years) 495  
between Se(VI) and Se(IV) may be inferred at low 496  
concentrations (i.e.,  $< 9 \mu\text{g/L}$ ) of Se(IV). In addition, 497  
Se(VI)–Se(IV) exchange may further be inhibited by removal 498  
of Se(IV) by either adsorption or by reduction to Se(0).<sup>11,39</sup> 499

#### Se Isotopes as Redox Indicators in the Unmined Area. 500

In addition to serving as an indicator for reduction of 501  
potentially toxic Se oxyanions in groundwater, the results 502  
from the unmined PAA 4 area demonstrate that stable Se 503  
isotope ratios aid in the precise determination of the redox state 504  
of the aquifer at Rosita ISR site (Table S1). Our previous work 505  
on U isotope ratios ( $^{238}\text{U}/^{235}\text{U}$ , expressed as  $\delta^{238}\text{U}$ )<sup>20</sup> showed 506  
evidence of U(VI) reduction in the transect containing MW 507  
158, BL 36, and MW 144 along the hydraulic gradient, 508  
particularly in the ore-zone BL and the down-gradient well, 509  
while there was a lack of U(VI)-reducing conditions along 510  
another transect (MW 154, BL 39, and MW 149) (Figure 2, 511  
Table S1). Along both transects, a decrease in  $\text{NO}_3^-$  in 512  
groundwater from  $\geq 12 \text{ mg/L}$  in the up-gradient wells to below 513  
detection in the ore-zone BL wells and down-gradient wells was 514  
also reported.<sup>20</sup> The western transect, where the lack of a large 515  
 $^{238}\text{U}$  depletion in groundwater indicated the absence of U(VI) 516  
reduction in the ore-zone well BL 39 ( $\delta^{238}\text{U} = 0.56\text{‰}$ ) and 517  
down-gradient MW 149 ( $\delta^{238}\text{U} = 0.48\text{‰}$ ) shows an overall 518  
enrichment in  $\delta^{82}\text{Se}$  of Se(VI) up to  $\sim 6\text{‰}$  relative to the 519  
average  $\delta^{82}\text{Se}$  ( $0.5\text{‰}$ ) of the U ore, with BL 39 exhibiting a 520  
 $\delta^{82}\text{Se}$  of  $6.14\text{‰}$ . This  $\delta^{82}\text{Se}$  of Se(VI) in BL 39 is  $\sim 4\text{‰}$  higher 521  
compared to that of the up-gradient well MW 154 ( $\delta^{82}\text{Se} =$  522  
 $2.19\text{‰}$ ). Se(VI) in the down-gradient well MW 149 is below 523  
the detection limit ( $< 0.1 \mu\text{g/L}$ ). This suggests progressively 524  
stronger Se(VI)-reducing conditions along the hydraulic 525  
gradient. 526

In comparison, the up-gradient well MW 158 ( $\delta^{238}\text{U} =$  527  
 $-0.08\text{‰}$ ) from the western transect shows  $^{82}\text{Se}$  depletion 528  
( $\delta^{82}\text{Se}_{\text{VI}} = -1.12\text{‰}$ ) with a lower Se(VI) concentration, 529  
suggesting spatial heterogeneity both in terms of background Se 530  
content and isotopic composition. However, the wells along the 531



532 hydraulic gradient in this transect with highly fractionated U  
533 isotope ratios, BL 36 ( $\delta^{238}\text{U} = -1.61\text{‰}$ ) and MW 144 ( $\delta^{238}\text{U}$   
534  $= -1.96\text{‰}$ ), have very little or no detectable Se oxyanions,  
535 suggesting almost-quantitative reduction of Se(VI) and Se(IV)  
536 removal of Se(IV) via adsorption onto aquifer material, or both.  
537 Thus, the results from the unmined PAA4 demonstrate the  
538 effectiveness of Se isotope ratios in delineating Se(VI)-reducing  
539 environments and in providing additional information about  
540 existing redox conditions that can not be obtained from the U  
541 isotopic data alone.

542 **Fractionation Mechanisms at Rosita and Comparison**  
543 **of  $\epsilon$  with Previous Studies.** The magnitude of the Se isotope  
544 fractionation observed at Rosita is more consistent with a  
545 microbial reduction mechanism than with abiotic reduction, but  
546 there is still sufficient uncertainty that abiotic reduction cannot  
547 be ruled out. Johnson et al. 2011 provides a detailed review of  
548 the magnitudes of Se isotope fractionation for various abiotic  
549 reductants and microbial species. Microbial reduction of Se  
550 oxyanions yields a range of  $\epsilon$  values spanning from  $-0.3\text{‰}$  to  
551  $-7.5\text{‰}$  for the reduction of Se(VI) to Se(IV) and from  
552  $-1.7\text{‰}$  to  $-12\text{‰}$  for the reduction of Se(IV) to Se(0). The  
553 abiotic reduction of Se generally yields consistently large  
554 ( $>-10\text{‰}$ ) isotopic fractionations. The  $\epsilon$  for reduction of  
555 Se(VI) to Se(IV) by the Fe(II)–Fe(III) layered double  
556 hydroxide mineral “green rust”, a likely reductant in soils and  
557 sediments, is  $\sim-11\text{‰}$ , while the reduction to Se(IV) to Se(0)  
558 by FeS and  $\text{NH}_2\text{OH}$  or ascorbic acid produces a fractionation  
559 (as  $\epsilon$ ) of  $-10\text{‰}$  and  $-15.0$  to  $-19.2\text{‰}$ , respectively. The  $\epsilon$   
560 determined from the groundwater samples from the Rosita ISR  
561 site ( $-2.25\text{‰} \pm 0.61\text{‰}$ ) is much smaller in comparison to that  
562 observed during abiotic Se(VI) reduction and falls within the  
563 range observed during Se(VI) reduction by natural microbial  
564 consortia.<sup>24</sup> Despite some heterogeneities, the observed  
565 sequence of redox reactions along the hydraulic gradient from  
566  $\text{NO}_3^-$  reducing to Fe(III)- and U(VI)-reducing environments is  
567 also consistent with the microbially mediated redox ladder in  
568 aquifers.<sup>40</sup> However, reservoir effects arising from the lack of  
569 chemical communication between the zones of reduction (e.g.,  
570 biofilms or mineral surfaces in clay-rich zones) and the bulk  
571 dissolved Se(VI) in the more rapidly flowing parts of the sandy  
572 aquifer may limit the expression of overall isotopic fractionation  
573 in groundwater samples and thus lead to a diminished apparent  
574  $\epsilon$  value.<sup>30</sup> Future research involving similar sites should be  
575 directed toward identification of the Se-reduction mechanism  
576 and determination of  $\epsilon$  at the site using analysis of the temporal  
577 trend of Se oxyanion concentrations with Se isotope ratios from  
578 the target wells. Additionally, the  $\epsilon$  determined from the field  
579 data should be complemented by laboratory experiments for  
580 the site-specific reduction mechanism.

581 **Implications for Monitoring of Se and U Reduction at**  
582 **ISR Sites.** The results of this study demonstrate that Se isotope  
583 ratios are effective indicators of natural attenuation of Se(VI), a  
584 residual product of ISR mining and a potential water  
585 contaminant for several ISR sites. Furthermore, our results  
586 suggest that the Se isotope ratios record the redox environ-  
587 ments precursory to U(VI)-reducing conditions that cannot be  
588 obtained from the concentration (e.g., Se(VI) or U(VI)) data  
589 alone.

590 A groundwater monitoring approach combining Se isotope  
591 ratios with U isotopic measurements is therefore advantageous  
592 in determining conditions conducive for post-mining natural  
593 attenuation of contaminants at ISR sites. For instance, naturally  
594 occurring aqueous and adsorbed Fe(II),<sup>41,42</sup> magnetite<sup>43,44</sup> and

titanomagnetite,<sup>45</sup> and FeS<sup>46,47</sup> (both residual after mining and  
595 biogenic) may readily reduce U(VI) in aquifers. These abiotic  
596 reductants are also capable of reducing Se(IV).<sup>48–51</sup> Thus, in  
597 addition to  $\delta^{238}\text{U}$ ,  $\delta^{82}\text{Se}$  of groundwater would provide an  
598 improved characterization of the existing redox state and  
599 reducing capacity of the aquifer. In aquifers with a need for  
600 active remediation, the knowledge of the existing redox state is  
601 also important to determine the remediation strategy and the  
602 choice of reductant (if used) to avoid aggressive reductive  
603 remediation, which may mobilize contaminants such as arsenic.  
604

Our measurements on Se speciation and stable Se isotopes  
605 reveal the spatial distribution at a single time and do not  
606 provide direct information on time-dependent changes in Se  
607 oxyanion concentrations and concomitant changes in Se  
608 isotope ratios. Efficient post-mining monitoring of reduction  
609 should include time-series measurements of Se oxyanion  
610 concentration and Se isotope ratios in samples from the target  
611 ore-zone BL wells or wells from the monitoring ring. This  
612 would enable more-accurate determination of the exact  
613 relationship between the changes in Se(VI) and Se(IV)  
614 concentrations in a target well and the associated shifts in  
615  $\delta^{82}\text{Se}$  (or the site-specific isotopic fractionation factor), which is  
616 required for the quantification of Se remediation.  
617

## ■ ASSOCIATED CONTENT

### 📄 Supporting Information

The Supporting Information is available free of charge on the  
620 ACS Publications website at DOI: [10.1021/acs.est.6b01464](https://doi.org/10.1021/acs.est.6b01464).  
621

Tables showing a comparison between Se(VI) and  
622 U(VI) concentrations in groundwater from PAA 4  
623 along with Se ( $\delta^{82}\text{Se}$ ) and U isotope ratios ( $\delta^{238}\text{U}$ ).  
624 Figures showing the correlation between  $\delta^{82}\text{Se}_{\text{IV}}$  and  
625 Se(IV) and the distribution of  $\text{NO}_3^-$  in Rosita ground-  
626 water. (PDF)  
627

## ■ AUTHOR INFORMATION

### Corresponding Author

\*Phone: +44 1784 443890; fax: +44 1784 471780; e-mail:  
630 [Anirban.Basu@rhl.ac.uk](mailto:Anirban.Basu@rhl.ac.uk).  
631

### Present Address

<sup>^</sup>A.B.: Department of Earth Sciences, Royal Holloway  
633 University of London, Egham Hill, Egham, Surrey, TW20  
634 OEX, United Kingdom.  
635

### Author Contributions

<sup>▽</sup>A.B. and K.S. contributed equally to this manuscript.  
637

### Notes

The authors declare no competing financial interest.  
639

## ■ ACKNOWLEDGMENTS

This research was funded by the UC Laboratory Fees Research  
641 Program. We thank Uranium Resources, Inc. for providing site  
642 access and logistic support during sample collection and  
643 drilling. The U.S. Department of Energy provided salary  
644 support for D.J.D. and J.N.C. during the study period under  
645 contract no. DE-AC02-05CH11231. We thank two anonymous  
646 reviewers and Associate Editor Daniel Giammar for con-  
647 structive comments that improved the quality of this manu-  
648 script.  
649



## 650 ■ REFERENCES

- 651 (1) Howard, J. H. Geochemistry of selenium: formation of ferroselite  
652 and selenium behavior in the vicinity of oxidizing sulfide and uranium  
653 deposits. *Geochim. Cosmochim. Acta* **1977**, *41* (11), 1665–1678.
- 654 (2) Dahlkamp, F. J. *Uranium deposits of the world*; Springer:  
655 Heidelberg, Germany, 2009.
- 656 (3) Granger, H. C.; Warren, C. G. Unstable sulfur compounds and  
657 the origin of roll-type uranium deposits. *Econ. Geol. Bull. Soc. Econ.*  
658 *Geol.* **1969**, *64* (2), 160–171.
- 659 (4) Xiong, Y. Predicted equilibrium constants for solid and aqueous  
660 selenium species to 300 °C: applications to selenium-rich mineral  
661 deposits. *Ore Geol. Rev.* **2003**, *23* (3–4), 259–276.
- 662 (5) Beath, O. A.; Hagner, A. F.; Gilbert, C. S. *Some rocks and soils of*  
663 *high selenium content*, Vol. 36; University of Wyoming: Laramie, WY,  
664 1946.
- 665 (6) Dribus, J. R.; Nanna, R. F. *National uranium resource evaluation,*  
666 *Rawlins quadrangle, Wyoming and Colorado*; Bendix Field Engineering  
667 Corp.: Grand Junction, CO, 1982.
- 668 (7) Plant, J. A.; Bone, J.; Voulovoulis, N.; Kinniburgh, D. G.; Smedley,  
669 P. L.; Fordyce, F. M.; Klinck, B. Arsenic and selenium. In *Treaties on*  
670 *Geochemistry*, 2nd ed.; Holland, H. D., Turekian, K. K., Eds.; Elsevier:  
671 Oxford, England, 2014; pp 13–57; [10.1016/B978-0-08-095975-](https://doi.org/10.1016/B978-0-08-095975-7.000902-5)  
672 [7.000902-5](https://doi.org/10.1016/B978-0-08-095975-7.000902-5).
- 673 (8) Bartz, G. L. Uranium prospecting based on selenium and  
674 molybdenum. US Patent Document 4,345,912/A; U.S. Commissioner  
675 of Patents, Washington, DC, 1982.
- 676 (9) Maher, K.; Bargar, J. R.; Brown, G. E., Jr. Environmental  
677 Speciation of Actinides. *Inorg. Chem.* **2013**, *52* (7), 3510–3532.
- 678 (10) Seby, F.; Potin-Gautier, M.; Giffaut, E.; Borge, G.; Donard, O. F.  
679 X. A critical review of thermodynamic data for selenium species at 25  
680 °C. *Chem. Geol.* **2001**, *171* (3–4), 173–194.
- 681 (11) Johnson, T. M. Stable Isotopes of Cr and Se as Tracers of Redox  
682 Processes in Earth Surface Environments. In *Handbook of environ-*  
683 *mental isotope geochemistry*; Baskaran, M., Ed.; Springer: Heidelberg,  
684 Germany, 2011; pp 155–175.
- 685 (12) Muscatello, J. R.; Belknap, A. M.; Janz, D. M. Accumulation of  
686 selenium in aquatic systems downstream of a uranium mining  
687 operation in northern Saskatchewan, Canada. *Environ. Pollut.* **2008**,  
688 *156* (2), 387–393.
- 689 (13) Muscatello, J. R.; Bennett, P. M.; Himbeault, K. T.; Belknap, A.  
690 M.; Janz, D. M. Larval Deformities Associated with Selenium  
691 Accumulation in Northern Pike (*Esox lucius*) Exposed to Metal  
692 Mining Effluent. *Environ. Sci. Technol.* **2006**, *40* (20), 6506–6512.
- 693 (14) Van Metre, P. C.; Gray, J. R. Effects of uranium mining  
694 discharges on water quality in the Puerco River basin, Arizona and  
695 New Mexico. *Hydro. Sci. J.* **1992**, *37* (5), 463–480.
- 696 (15) Williams, K. H.; Wilkins, M. J.; N'Guessan, A. L.; Arey, B.;  
697 Dodova, E.; Dohnalkova, A.; Holmes, D.; Lovley, D. R.; Long, P. E.  
698 Field evidence of selenium bioreduction in a uranium-contaminated  
699 aquifer. *Environ. Microbiol. Rep.* **2013**, *5* (3), 444–452.
- 700 (16) OECD Nuclear Energy Agency; International Atomic Energy  
701 Agency. *Resources, Production and Demand*; A joint report by the  
702 OECD; Nuclear Energy Agency and the International Atomic Energy  
703 Agency: Paris, France, 2012; [http://www.oecd-nea.org/ndd/pubs/](http://www.oecd-nea.org/ndd/pubs/2012/7059-uranium-2011.pdf)  
704 [2012/7059-uranium-2011.pdf](http://www.oecd-nea.org/ndd/pubs/2012/7059-uranium-2011.pdf).
- 705 (17) OECD Nuclear Energy Agency; International Atomic Energy  
706 Agency. *Resources, Production and Demand*; A joint report by the  
707 OECD. Nuclear Energy Agency and the International Atomic Energy  
708 Agency: Paris, France, 2014; [https://www.oecd-nea.org/ndd/pubs/](https://www.oecd-nea.org/ndd/pubs/2014/7209-uranium-2014.pdf)  
709 [2014/7209-uranium-2014.pdf](https://www.oecd-nea.org/ndd/pubs/2014/7209-uranium-2014.pdf).
- 710 (18) Ramirez, P., Jr.; Rogers, B. P. Selenium in a Wyoming Grassland  
711 Community Receiving Wastewater from an In Situ Uranium Mine.  
712 *Arch. Environ. Contam. Toxicol.* **2002**, *42* (4), 431–436.
- 713 (19) Davis, J. A.; Curtis, G. P. Consideration of geochemical issues in  
714 groundwater restoration at uranium in-situ leach mining facilities  
715 (NUREG/CR-6870); Report for the Division of Fuel, Engineering,  
716 and Radiological Research, Office of Nuclear Regulatory Research, US  
717 Nuclear Regulatory Commission; Washington, DC, 2007.
- (20) Basu, A.; Brown, S. T.; Christensen, J. N.; DePaolo, D. J.; 718  
Reimus, P. W.; Heikoop, J. M.; Woldegabriel, G.; Simmons, A. M.; 719  
House, B. M.; Hartmann, M.; Maher, K. Isotopic and Geochemical 720  
Tracers for U(VI) Reduction and U Mobility at an In Situ Recovery U 721  
Mine. *Environ. Sci. Technol.* **2015**, *49* (10), 5939–5947. 722
- (21) Brown, S. T.; Basu, A.; Christensen, J. N.; Reimus, P. W.; 723  
Heikoop, J. M.; Simmons, A. M.; WoldeGabriel, G.; Maher, K.; 724  
Weaver, K.; Clay, J.; DePaolo, D. J. Isotopic evidence for reductive 725  
immobilization of uranium across a roll-front mineral deposit. *Environ.* 726  
*Sci. Technol.* **2016**, *50*, 6189. 727
- (22) Johnson, T. M.; Bullen, T. D. Mass-Dependent Fractionation of 728  
Selenium and Chromium Isotopes in Low-Temperature Environ- 729  
ments. *Rev. Mineral. Geochem.* **2004**, *55* (1), 289–317. 730
- (23) Johnson, T. M.; Bullen, T. D. Selenium isotope fractionation 731  
during reduction by Fe (II)-Fe (III) hydroxide-sulfate (green rust). 732  
*Geochim. Cosmochim. Acta* **2003**, *67* (3), 413–419. 733
- (24) Ellis, A. S.; Johnson, T. M.; Herbel, M. J.; Bullen, T. D. Stable 734  
isotope fractionation of selenium by natural microbial consortia. *Chem.* 735  
*Geol.* **2003**, *195* (1–4), 119–129. 736
- (25) Herbel, M. J.; Johnson, T. M.; Oremland, R. S.; Bullen, T. D. 737  
Fractionation of selenium isotopes during bacterial respiratory 738  
reduction of selenium oxyanions. *Geochim. Cosmochim. Acta* **2000**, 739  
*64* (21), 3701–3709. 740
- (26) Mitchell, K.; Couture, R.-M.; Johnson, T. M.; Mason, P. R. D.; 741  
Van Cappellen, P. Selenium sorption and isotope fractionation: 742  
Iron(III) oxides versus iron(II) sulfides. *Chem. Geol.* **2013**, *342* (C), 743  
21–28. 744
- (27) Johnson, T. M.; Herbel, M. J.; Bullen, T. D.; Zawislanski, P. T. 745  
Selenium isotope ratios as indicators of selenium sources and oxyanion 746  
reduction. *Geochim. Cosmochim. Acta* **1999**, *63* (18), 2775–2783. 747
- (28) Schilling, K.; Johnson, T. M.; Mason, P. R. D. A sequential 748  
extraction technique for mass-balanced stable selenium isotope 749  
analysis of soil samples. *Chem. Geol.* **2014**, *381* (C), 125–130. 750
- (29) Schilling, K.; Johnson, T. M.; Dhillon, K. S.; Mason, P. R. D. 751  
Fate of selenium in soils at a seleniferous site recorded by high 752  
precision Se isotope measurements. *Environ. Sci. Technol.* **2015**, *49* 753  
(16), 9690–9698. 754
- (30) Clark, S. K.; Johnson, T. M. Effective Isotopic Fractionation 755  
Factors for Solute Removal by Reactive Sediments: A Laboratory 756  
Microcosm and Slurry Study. *Environ. Sci. Technol.* **2008**, *42* (21), 757  
7850–7855. 758
- (31) Carignan, J.; Wen, H. Scaling NIST SRM 3149 for Se isotope 759  
analysis and isotopic variations of natural samples. *Chem. Geol.* **2007**, 760  
*242* (3–4), 347–350. 761
- (32) Hyslop, N. P.; White, W. H. Estimating Precision Using 762  
Duplicate Measurements. *J. Air Waste Manage. Assoc.* **2009**, *59* (9), 763  
1032–1039. 764
- (33) Scott, K. M.; Lu, X.; Cavanaugh, C. M.; Liu, J. S. Optimal 765  
methods for estimating kinetic isotope effects from different forms of 766  
the Rayleigh distillation equation. *Geochim. Cosmochim. Acta* **2004**, *68* 767  
(3), 433–442. 768
- (34) Reynolds, R. L.; Goldhaber, M. B. Iron disulfide minerals and 769  
the genesis of roll-type uranium deposits. *Econ. Geol. Bull. Soc. Econ.* 770  
*Geol.* **1983**, *78* (1), 105–120. 771
- (35) Reynolds, R. L.; Goldhaber, M. B. Origin of a South Texas Roll- 772  
Type Uranium Deposit 0.1. Alteration of Iron-Titanium Oxide 773  
Minerals. *Econ. Geol. Bull. Soc. Econ. Geol.* **1978**, *73* (8), 1677–1689. 774
- (36) Huang, W. H. Geochemical and sedimentologic problems of 775  
uranium deposits of Texas Gulf Coastal Plain. *AAPG Bull.* **1978**, *62*, 776  
1049–1062. 777
- (37) Granger, H. C. Ferroselite in a roll-type uranium deposit, 778  
Powder River Basin, Wyoming. *U.S. Geological Survey Professional* 779  
*Paper* **1966**, C133–C137. 780
- (38) Wang, X.; Johnson, T. M.; Lundstrom, C. C. Low temperature 781  
equilibrium isotope fractionation and isotope exchange kinetics 782  
between U(IV) and U(VI). *Geochim. Cosmochim. Acta* **2015**, *158*, 783  
262–275. 784
- (39) White, A. F.; Benson, S. M.; Yee, A. W.; Wollenberg, H. A.; 785  
Flexser, S. Groundwater contamination at the Kesterson Reservoir, 786

- 787 California: 2. Geochemical parameters influencing selenium mobility.  
788 *Water Resour. Res.* **1991**, *27* (6), 1085–1098.
- 789 (40) McMahon, P. B.; Chapelle, F. H. Redox Processes and Water  
790 Quality of Selected Principal Aquifer Systems. *Groundwater* **2008**, *46*  
791 (2), 259–271.
- 792 (41) Du, X.; Boonchayaanant, B.; Wu, W.-M.; Fendorf, S.; Bargar, J.;  
793 Criddle, C. S. Reduction of Uranium(VI) by Soluble Iron(II)  
794 Conforms with Thermodynamic Predictions. *Environ. Sci. Technol.*  
795 **2011**, *45* (11), 4718–4725.
- 796 (42) Taylor, S. D.; Marcano, M. C.; Rosso, K. M.; Becker, U. An  
797 experimental and ab initio study on the abiotic reduction of uranyl by  
798 ferrous iron. *Geochim. Cosmochim. Acta* **2015**, *156*, 154–172.
- 799 (43) Latta, D. E.; Gorski, C. A.; Boyanov, M. I.; O'Loughlin, E. J.;  
800 Kemner, K. M.; Scherer, M. M. Influence of Magnetite Stoichiometry  
801 on U<sup>VI</sup> Reduction. *Environ. Sci. Technol.* **2012**, *46* (2), 778–786.
- 802 (44) Yuan, K.; Renock, D.; Ewing, R. C.; Becker, U. Uranium  
803 reduction on magnetite: Probing for pentavalent uranium using  
804 electrochemical methods. *Geochim. Cosmochim. Acta* **2015**, *156*, 194–  
805 206.
- 806 (45) Latta, D. E.; Pearce, C. I.; Rosso, K. M.; Kemner, K. M.;  
807 Boyanov, M. I. Reaction of U<sup>VI</sup> with Titanium-Substituted Magnetite:  
808 Influence of Ti on U<sup>IV</sup> Speciation. *Environ. Sci. Technol.* **2013**, *47* (9),  
809 4121–4130.
- 810 (46) Veeramani, H.; Scheinost, A. C.; Monsegue, N.; Qafoku, N. P.;  
811 Kukkadapu, R.; Newville, M.; Lanzirrotti, A.; Pruden, A.; Murayama,  
812 M.; Hochella, M. F., Jr. Abiotic Reductive Immobilization of U(VI) by  
813 Biogenic Mackinawite. *Environ. Sci. Technol.* **2013**, *47* (5), 2361–2369.
- 814 (47) Troyer, L. D.; Tang, Y.; Borch, T. Simultaneous Reduction of  
815 Arsenic(V) and Uranium(VI) by Mackinawite: Role of Uranyl  
816 Arsenate Precipitate Formation. *Environ. Sci. Technol.* **2014**, *48* (24),  
817 14326–14334.
- 818 (48) Myneni, S.; Tokunaga, T. K.; Brown, G. E. Abiotic selenium  
819 redox transformations in the presence of Fe(II,III) oxides. *Science*  
820 **1997**, *278* (5340), 1106–1109.
- 821 (49) Scheinost, A. C.; Charlet, L. Selenite Reduction by Mackinawite,  
822 Magnetite and Siderite: XAS Characterization of Nanosized Redox  
823 Products. *Environ. Sci. Technol.* **2008**, *42* (6), 1984–1989.
- 824 (50) Charlet, L.; Scheinost, A. C.; Tournassat, C.; Greneche, J. M.;  
825 Géhin, A.; Fernández-Martínez, A.; Coudert, S.; Tisserand, D.;  
826 Brendle, J. Electron transfer at the mineral/water interface: Selenium  
827 reduction by ferrous iron sorbed on clay. *Geochim. Cosmochim. Acta*  
828 **2007**, *71* (23), 5731–5749.
- 829 (51) Baik, M. H.; Lee, S. Y.; Jeong, J. Sorption and reduction of  
830 selenite on chlorite surfaces in the presence of Fe(II) ions. *J. Environ.*  
831 *Radioact.* **2013**, *126*, 209–215.